Environmental Research 109 (2009) 721–727

Contents lists available at ScienceDirect

Environmental Research

journal homepage: www.elsevier.com/locate/envres

Atmospheric mercury in Changbai Mountain area, northeastern China II. The distribution of reactive gaseous mercury and particulate mercury and mercury deposition fluxes ☆

Qi Wan [a,b], Xinbin Feng [a,*], Julia Lu [c,*], Wei Zheng [a,b], Xinjie Song [c], Ping Li [a,b], Shijie Han [d], Hao Xu [d]

[a] State Key Laboratory of Environmental Geochemistry, Institute of Geochemistry, Chinese Academy of Sciences, Guiyang 550002, PR China
[b] Graduate University of Chinese Academy of Sciences, Beijing 100049, PR China
[c] Department of Chemistry and Biology, Ryerson University, Toronto, Ont., Canada M5B 2K3
[d] Open Research Station of Changbai Mountain Forest Ecosystems, Chinese Academy of Sciences, Yanbian 133613, PR China

ARTICLE INFO

Article history:
Received 11 October 2008
Received in revised form
18 May 2009
Accepted 26 May 2009
Available online 13 June 2009

Keywords:
Reactive gaseous mercury
Particulate mercury
Total mercury
Wet deposition flux
Dry deposition flux

ABSTRACT

Reactive gaseous mercury (RGM) and particulate mercury (Hgp) concentrations in ambient air from a remote site at Changbai Mountain area in northeastern China were intermittently monitored from August 2005 to July 2006 totaling 93 days representing fall, winter–spring and summer season, respectively. Rainwater and snow samples were collected during a whole year, and total mercury (THg) in rain samples were used to calculate wet depositional flux. A throughfall method and a model method were used to estimate dry depositional flux. Results showed mean concentrations of RGM and Hgp are 65 and 77 pg m^{-3}. Compared to background concentrations of atmospheric mercury species in Northern Hemisphere, RGM and Hgp are significantly elevated in Changbai area. Large values for standard deviation indicated fast reactivity and a low residence time for these mercury species. Seasonal variability is also important, with lower mercury levels in summer compared to other seasons, which is attributed to scavenging by rainfall and low local mercury emissions in summer. THg concentrations ranged from 11.5 to 15.9 ng L^{-1} in rainwater samples and 14.9–18.6 ng L^{-1} in throughfall samples. Wet depositional flux in Changbai area is calculated to be 8.4 μg m^{-2} a^{-1}, and dry deposition flux is estimated to be 16.5 μg m^{-2} a^{-1} according to a throughfall method and 20.2 μg m^{-2} a^{-1} using a model method.

1. Introduction

Mercury (Hg) is a highly toxic heavy metal and is considered a global pollutant due to its ability to undergo long distance transport in the atmosphere. It is emitted into the atmosphere by various anthropogenic and natural sources. Atmospheric Hg consists of three different physical and chemical forms, including gaseous elemental Hg (GEM), reactive gaseous Hg (RGM), and particulate Hg (Hgp) (Lindberg and Stratton, 1998). RGM and Hgp from anthropogenic and natural sources are introduced into terrestrial and aquatic ecosystems via wet and dry deposition (Mason and Sullivan, 1997; Landis and Keeler, 2002). Recent studies reported RGM may represent 1–3% of total gaseous Hg (T_{GM}) at rural continental sites (Lindberg and Stratton, 1998; Landis et al., 2002; Poissant et al., 2004). Because RGM is highly reactive and rapidly scavenged by moist particles and surfaces, it can fall off quickly with distance from their primary sources (e.g., incinerators, non-metal smelters and power plants) (Lindberg and Stratton, 1998). Thus, RGM concentrations are likely to be highly variable and related to point sources, meteorological conditions and oxidant levels in the air. Hgp is associated with airborne particles, such as dust, soot, sea-salt aerosols, ice crystal or is likely produced by adsorption of RGM species (e.g., $HgCl_2$) onto atmospheric particles (Lu and Schroeder, 2004).

Even though RGM and Hgp represent a small proportion of total Hg in the atmosphere, they are crucial in Hg transport and removal processes (Lindberg and Stratton, 1998). The most important characteristic of RGM is its high water solubility, and this allows its dissolution in rainwater and subsequent wet deposition. Most of this deposited Hg is reemitted to the atmosphere, and a small amount is converted to methyl Hg and bio-accumulates in water or fish, causing serious damage to the environment (US EPA et al., 2001). Although anthropogenic emissions of Hg are decreasing in industrialized countries due to emission controls, efficiency improvements, and environmental stewardship, globally total anthropogenic Hg emissions appear to

Abbreviations: RGM, reactive gaseous mercury; Hgp, particulate mercury; TGM, total gaseous mercury; THg, total mercury; F_w, wet deposition flux; F_d, dry deposition flux; C_R, THg in rainwater; C_T, THg in throughfall; C_{Hgp}, concentration of particulate mercury; P^i, precipitation amount in rain sample; P_{Tf}, precipitation in throughfall sample; τ, dry deposition time; v_d, dry depositional velocity

☆ Funding sources: The study is financially supported by Natural Science Foundation of China (405320514) and Chinese Academy of Sciences through an International Partnership Project.

* Corresponding authors. Fax: +86 851 5891609.
E-mail addresses: fengxinbin@vip.skleg.cn (X. Feng), Julialu@ryerson.ca (J. Lu).

0013-9351/$ - see front matter © 2009 Elsevier Inc. All rights reserved.
doi:10.1016/j.envres.2009.05.006

be increasing (Pacyna and Pacyna, 2002). Spatial gradients of Hg deposition are largely caused by significant contributions of Hg emissions from urban/industrial regions, where concentrations of Hg species (GEM, RGM and Hgp), particularly concentrations of RGM and Hgp, are much higher and more variable than in rural areas (Landis and Keeler, 2002).

In recent years, more studies concerning the concentration, distribution and chemical speciation of Hg in atmosphere were conducted due to considerable advances in analytical techniques for measuring Hg species. In addition, estimating the contribution of precipitation scavenging of RGM and Hgp is important for understanding the causes of seasonal and regional variations of Hg wet and dry deposition. Studies have shown that wet depositional flux estimates based on direct and indirect measurements ranged from 5 to 16 $\mu g\,m^{-2}\,a^{-1}$ in North America during 1980s (Fitzgerald et al., 1991; Swain et al., 1992), 5.8–18 $\mu g\,m^{-2}\,a^{-1}$ in some Japanese areas (Sakata and Asakura, 2007), and 3–30 $\mu g\,m^{-2}\,a^{-1}$ in North America in early 2000s (Ericksen et al., 2005). China is now regarded as one of the largest Hg emission countries in the world (Streets et al., 2005; Wu et al., 2006), and elevated Hg concentrations in the air causes Hg contamination in remote areas via transport followed by wet and dry deposition. Examples of regional and global models currently used to study the fate of Hg species and depositional fluxes in the atmosphere include the Hybrid Single Particle Lagrangian Integrated Trajectory (HYSPLIT) Model, Version 4) (Cohen et al., 2004), and the Eulerian Model for Air Pollution (EMAP) (Ryaboshapko et al., 2002). However, the concentrations of Hg species and subsequent depositional fluxes produced by these models are quite different from the values obtained by the field-monitoring campaigns (Fu et al., 2008). In order to evaluate the performance of current global atmospheric models, more measurement campaigns are needed at different geographical locations (Lindberg et al., 2007); however, data on Hg concentrations, speciation in ambient air and depositional fluxes in China are scarce, which hinders our understanding of Hg speciation cycling in the atmosphere and the environmental impacts. Here for the first time we evaluated Hg speciation and depositional fluxes in northeastern China for better understanding of Hg cycling in the environment.

2. Materials and methods

2.1. Study area and sampling site

The details of the sampling site were described in our companion paper (Wan et al., 2009). Briefly, Changbai Mountain (42°24′N, 128°28′E) is in the eastern Jilin Province, northeastern China, which is near the boundary between China and North Korea. It has a hilly terrain with altitudes ranging from 500 to 2700 m above sea level. The regional topography is characterized by forests and mountains. Changbai Mountain area is in the North Temperate Zone with abundant precipitation in summer and low temperature in winter. It is surrounded by a forest ecosystem and there are no large industrial utilities nearby.

The sampling site locates at the Research Station of Changbai Mountain Forest Ecosystems, Chinese Academy of Sciences, which is situated 5 km away from the nearest town, Baihe, near Yanji City in Jilin Province. RGM and Hgp sampling campaigns were carried out 2 m above the roof of a building, a total of 5 m above the ground, using air inlet of Teflon tubing. Measurements were intermittently performed from 5 August 2005 to 5 July 2006, including three intensive periods to characterize the RGM and Hgp distribution. Sampling campaigns are (1) from 10 August to 27 September 2005, (2) from 23 February to 11 March 2006, and (3) from 6 June to 5 July 2006, respectively. Three periods occurred during fall, winter–spring and summer. A total of 1005 samples during 93 days were collected.

2.2. Atmospheric Hg species sampling and analysis

Automated Hg speciation analyzer systems were used concurrently during the field measurement study. Analyzer systems included a Tekran Model 2537A were used together with a Model 1130 Speciation Unit and a Model 1135 Hgp Unit to simultaneously monitor RGM and Hgp (0.1–2.5 μm) in ambient air (Tekran, 2001). The systems allow a fully automated operation with all three Hg components being concurrently measured. RGM in the atmosphere is captured in a Model 1130 KCl-coated quartz annular denuder module during sampling, while Hgp is trapped onto a unique quartz regenerable filter located within Model 1135. RGM and Hgp components are then sequentially desorbed during the analysis phase. Both units are configured to collect 1 h samples at a 10 $L\,min^{-1}$ flow rate. After 1 h sampling period, 1130 and 1135 systems are flushed with Hg-free air during the next 1 h period, and RGM and Hgp are sequentially thermodesorbed and analyzed. Thus, RGM and Hgp collected are thermally decomposed into an Hg-free air stream and subsequently analyzed by 2537A, respectively. Sampling and analyzing cycle is 2 h for RGM and Hgp. The quartz filter collects fine particles ($<$0.1–2.5 μm) whereas the denuders collect oxidized RGM compounds with a diffusion coefficient $>0.1\,cm^2\,s^{-1}$ that readily adheres to a KCl coating at 50 °C (Landis et al., 2002). Hence, some Hgp fractions larger than 2.5 μm are missing in this study. Denuders and regenerable particulate filters (RPF) were reconditioned and biweekly changed using a Tekran protocol, and quality control of Hg data was conducted by both automatic and manual calibration towards to Tekran Model 2537A followed by the operation manual (Tekran, 2001).

2.3. Wet and dry deposition

2.3.1. Rainfall and throughfall collection

All the rainfall, snowfall and throughfall samples were collected in the whole sampling periods to investigate mercury deposition flux. Rain sampling was conducted in a national meteorological field near the atmospheric Hg species sampling site, while throughfall sampling was carried out in an ecological sample area under a canopy of typical trees in northeastern China. Generally, we selected trees with broadleaves and conifers to obtain THg duplicate samples based on the throughfall method described by Lindberg and co-workers (1992). Both precipitation and throughfall samples were carried out approximately 1.5 m above the soil surface and far away from any obvious anthropogenic disturbances or Hg contamination. Two kinds of rain samples were collected using the same type of container: a bulk sampler with an acid-washed borosilicate glass bottle and a borosilicate glass wide-mouthed (15 cm in diameter) jar supported in a poly-vinyl chloride housing system supplied by our ultra-clean lab (Oslo and Paris Commission, 1998). After rainwater samples were collected, acidified and then shipped in Teflon bottles to our laboratory for analysis, which generally consisted of a digestion step with an acid solution of bromine chloride (BrCl), a pre-reduction step with hydroxylamine hydrochloride ($NH_2OH\cdot HCl$) solution and stannous chloride ($SnCl_2\cdot 2H_2O$), and then the reduced Hg vapor is analyzed by dual gold amalgamation followed by CVAFS quantification (US EPA et al., 2001). THg determination was conducted with the method blank and duplicates. Here, the method detection limit (MDL), based on three times the standard deviation of replicate measurements of a blank solution is 0.02 $ng\,L^{-1}$ and the method blank is found to be obviously under the detection limits in all cases. The average standard deviation on precision test for the duplicate samples analysis of THg is 4.5%. Spike recoveries for THg were between 93% and 110%.

2.3.2. Calculation the dry/wet deposition flux

Calculation of wet depositional flux of atmospheric Hg according to THg concentration in rainfall is based on Eq. (1):

$$F_w = \frac{1}{1000}\sum_{i=1}^{i=12}(C_R^i P^i) \quad (1)$$

where F_w is wet depositional flux ($\mu g\,m^{-2}\,a^{-1}$), C_R is THg in rainwater ($ng\,L^{-1}$), and the precipitation amount associated with each sample is indicated by P^i (mm).

Dry depositional fluxes can be obtained by direct determination and estimation using theoretical models. A multiple resistance model developed by Hicks et al. (1987) and modified by Lindberg et al. (1992) is used to determine depositional flux in a forest canopy as shown in Eq. (2).

$$F_d = \frac{1}{1000}\sum_{i=1}^{i=12}\left[(C_T^i - C_R^i)\frac{P_{Tf}^i}{\tau^i}\right] \quad (2)$$

where F_d is the dry deposition flux ($\mu g\,m^{-2}\,a^{-1}$), C_T is THg in throughfall ($ng\,L^{-1}$), C_R is the same as Eq. (1), the precipitation associated with each sample is indicated by P_{Tf} (mm), and τ is dry deposition time (h) (Lindberg et al., 1994). In comparison, we present a modeled method to calculate the dry depositional flux. A dry depositional flux model is widely used as shown in Eq. (3) (Fitzgerald et al., 1991; Pirrone et al., 1995):

$$F_d = C_{Hgp}\,v_d \quad (3)$$

where F_d is dry depositional flux ($\mu g\,m^{-2}\,a^{-1}$), v_d is the dry depositional velocity of particulate Hg ($cm\,s^{-1}$) and C_{Hgp} is the concentration of ambient particulate Hg.

3. Results and discussion

3.1. Overall RGM and Hgp concentrations

Fig. 1 depicts hourly RGM and Hgp concentrations during the sampling campaigns. RGM (0–880 pg m^{-3}) and Hgp (0–1001 pg m^{-3}) both exhibited a strong temporal variability among seasons as well as within the same season. Spikes of high RGM and Hgp concentrations were frequently observed, indicating different Hg emission sources, which resulted in high variability within the dataset. Fig. 2 shows the diurnal distribution of Hg species. Here, a pronounced diurnal variation was observed for RGM and Hgp levels, which suggested that RGM, like other daytime species such as ozone, generally peaks from midday to early afternoon when photochemical production is the greatest, and is rapidly removed by nocturnal dry deposition (Lindberg and Stratton, 1998; Poissant et al., 2005; Liu et al., 2007). Poissant et al. (2005) reported that Hgp shared a similar diurnal pattern with RGM instead of with GEM as seen in our study. Gabriel et al. (2005) found Hgp shared a similar diurnal pattern with RGM but only at a rural site. These results suggested that Hg species in rural areas have a different distribution pattern compared to urban areas because source types, surface characteristics, and meteorological conditions are different. This temporal variability of RGM and Hgp species may have considerable impacts on subsequent deposition, highlighting the importance of conducting measurements of RGM and Hgp in remote areas. A more pronounced diurnal trend was observed for RGM than Hgp, especially in winter–spring and during the later summer as shown in Fig. 1. Amazingly, there were very low RGM/Hgp concentration episodes in late fall and early summer, in which Hgp levels are under the limit of detection.

Table 1 includes a statistical summary of RGM and Hgp concentrations for the three seasons. Mean RGM and Hgp were 65 and 77 pg m^{-3}, which were comparable to other studies using similar instrumentation in Europe, North America and Arctic area (Berg et al., 2003). Poissant et al. (2005) measured values between 0 and 386 pg m^{-3} for RGM and 0–1528 pg m^{-3} for Hgp in southern Québec; Han et al. (2004) measured RGM values up to 90 pg m^{-3} in New York; Sheu and Mason (2001) reported RGM of 15–40 pg m^{-3} in Maryland; and levels were also comparable with those measured in Mt. Gongga in Southwestern China (Fu et al., 2008) and some areas in Japan (Sakata and Marumoto, 2005).

RGM and Hgp concentrations showed a seasonal variability. RGM concentrations were 62 ± 87 pg m^{-3} in non-heating seasons (fall and summer) and 84 ± 66 pg m^{-3} in heating season (winter–spring); while Hgp concentrations were 60 ± 115 pg m^{-3} during the warm seasons (fall and summer) and 167 ± 184 pg m^{-3} during the cold season (winter–spring). This obvious variation of RGM and Hgp indicatesd a faster reactivity and a lower residence time in the air. Hgp was obviously elevated in winter–spring season.

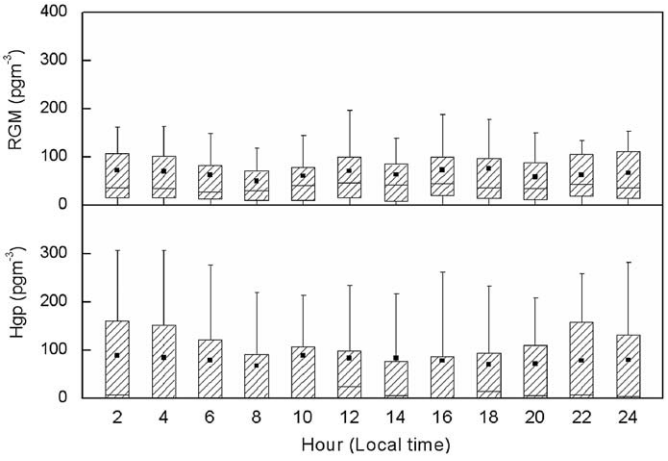

Fig. 2. Diurnal variation of Hg species in Changbai area for the whole sampling periods. (The lower boundary of the box indicates the 25th percentile, a line within the box marks the median, the black dot in the box shows the mean value and the upper boundary of the box indicates the 75th percentile. Whiskers above and below the box depict the 90th and 10th percentiles, respectively).

Table 1
Statistical summary of RGM and Hgp concentrations (pg m^{-3}) in Changbai Mountain area.

	Sampling periods	*N*	Min–Max	Mean	Median	SD
RGM	(1) 05-8-10–05-9-27	499	0–880	83	58	102
	(2) 06-2-23–06-3-11	182	0–472	84	72	66
	(3) 06-6-6–06-7-5	324	0–585	29	25	37
	Total	1005	0–880	65	38	84
Hgp	(1) 05-8-10–05-9-27	499	0–945	89	0	136
	(2) 06-2-23–06-3-11	182	0–1001	167	118	184
	(3) 06-6-6–06-7-5	324	0–606	15	0	40
	Total	1005	0–1001	77	5	136

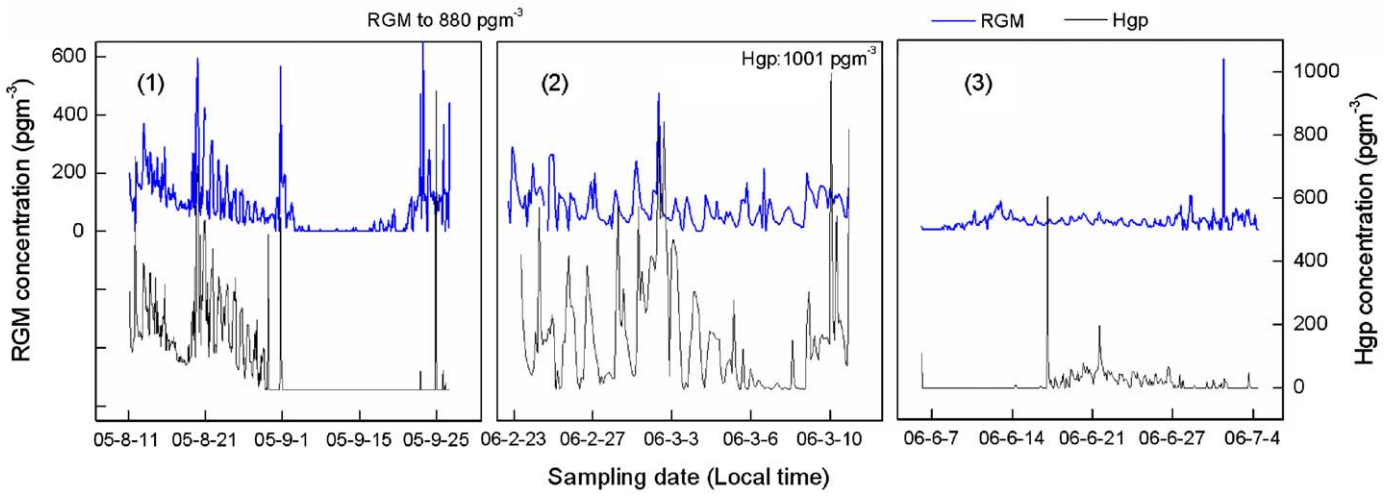

Fig. 1. RGM and Hgp concentrations in the air of Changbai Mountain area; Hourly RGM/Hgp concentrations during three study periods from August 2005 to July 2006.

This is probably due to local and regional biofuel and coal burning for domestic use. TGM levels in spring/winter were relatively high and stable compared to summer/fall in Changbai area (Wan et al., 2009). This strongly suggested that local and regional human activities significantly impacted the distribution of RGM and Hgp.

Levels for Hg species in the Changbai area were much lower in the summer compared to other seasons, and were synchronous with TGM. Rainfall scavenging may be a crucial factor. Studies showed that RGM and Hgp may be washed out by rain because of their high water solubility (Mason et al., 1997; Sakata and Asakura, 2007). It is also likely the source of Hg species varied in different seasons due to domestic coal burning for house heating during the colder period.

3.2. Wind directional dependence and potential Hg sources

RGM and Hgp are emitted by various sources, and concentrations in ambient air are largely varied dependent on the direct emissions of local and regional sources and in situ formation in the atmosphere (Sakata and Asakura, 2007). It is difficult to characterize source–receptor relationships, including meteorological effects, on the ambient Hg species in the study area due to the complex mixture of regional or long-range transport of anthropogenic Hg sources. Here, we characterize the wind direction dependence to identify conditions associated with elevated Hg species concentrations.

Fig. 3 shows the mean RGM and Hgp levels for wind direction, which are sorted into 22.5° sectors, so that each sector represents a large number of observations. In general, RGM and Hgp concentrations are enhanced by winds from any direction, compared to some background areas in North America and Europe (Sheu and Mason, 2001; Poissant et al. 2005). Atmospheric Hg sources (for GEM) in the study area are from coal, biofuel combustion and long-range transport by wind (Wan et al., 2009). Additionally, winds from 0–135° and 225°–315° carried more RGM and Hgp than wind from other directions. Wan et al. (2009) reported that Baihe town situated northwest to northeast from the sampling site is a densely residential area and winds passing over this area carried high RGM and Hgp concentrations exceeding mean values, especially in the cold season. It is estimated that in China total annual man-made Hg emissions were about 536 tons, of which 62.1% is attributed to coal combustion in 1999 (Streets et al., 2005). Hence, anthropogenic emissions from domestic coal burning for house heating and/or living and Hg emissions transported by wind are primary sources of atmospheric Hg.

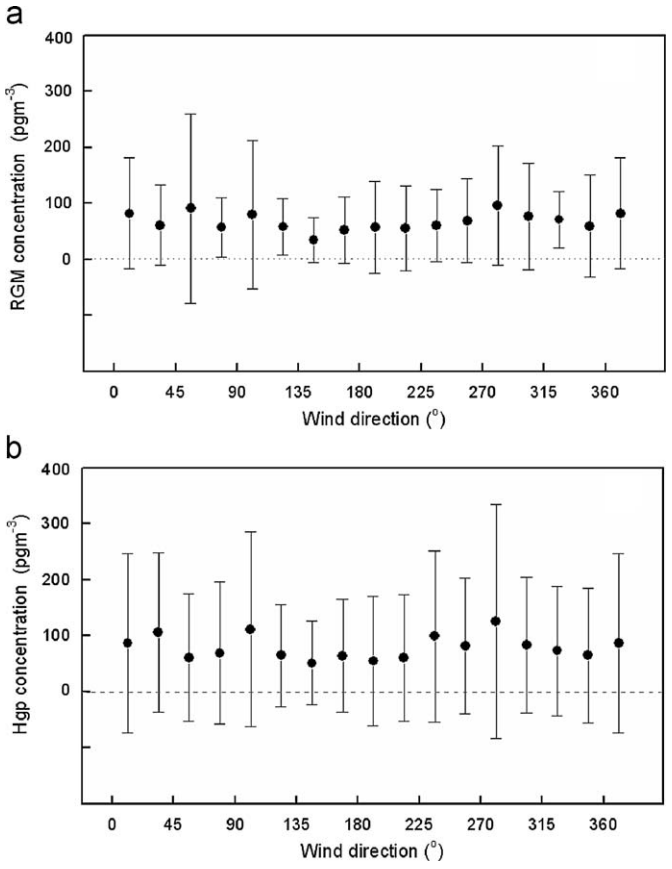

Fig. 3. Wind directional dependence of RGM (a) and Hgp (b) data for the whole sampling periods.

Table 2 lists four underlying factors (with eigenvalues >1) resulted from PCA model, which can be classified as three main aspects: diurnal mixing, source contributions, and seasonal meteorological conditions. Factor 1 has a strong positive loading for wind speed and solar radiation, but a strong negative loading for relative humidity. The loadings on meteorological variables may indicate daytime Hg photochemistry production (Hg^0–Hg^{2+}) as well as particulate adsorption and long-range transport by wind (air mass). Factor 2 only shows a strong negative loading with air temperature and a moderate positive correlation with air pressure. Factors 3 and 4 have strong positive correlations with all three Hg species, which suggests regional Hg emissions. It is also showed that RGM is significantly correlated with Hgp ($r=0.872$, $p<0.001$) according to a correlation analysis, which implied a common Hg source for both RGM and Hgp. RGM and Hgp are also significantly negatively correlated with wind speed, which suggested the impacts of local anthropogenic sources. RGM and Hgp did not show a distinct correlation with TGM ($r=0.087/0.052$, $p=0.014/0.147$). However, only during the sampling campaign in fall, significant correlations between TGM and RGM/Hgp were obtained ($r=0.483/0.515$, $p<0.001$), and this may indicate the Hg species shared a common anthropogenic source.

3.3. Wet and dry deposition fluxes

Hg is a pollutant of concern primarily due to its bioaccumulation in aquatic environments, although atmospheric deposition is a major input route (Mason et al., 1997; Landis and Keeler, 2002). Deposition of gaseous elemental Hg (>95% of the total) is ignored because of its extremely low solubility in water (Sakata and Marumoto, 2005), while RGM and Hgp are regarded as main sources for Hg deposition.

Table 2
Results from principal component analysis (PCA) model.

Variables	Factor 1	Factor 2	Factor 3	Factor 4
RGM	0.25	0.32	0.58	−0.04
Hgp	0.24	0.32	0.53	−0.27
TGM	0.14	0.24	0.06	0.55
T	−0.10	−0.55	0.38	0.16
WD	0.18	0.06	−0.24	−0.51
WS	0.46	−0.10	−0.21	−0.34
SR	0.43	−0.47	0.14	0.20
P	0.27	0.40	−0.32	0.42
RH	−0.59	0.20	0.14	−0.10
Eigenvalues	2.08	1.76	1.29	1.18
Variance explained (%)	23.2	19.5	14.4	13.1

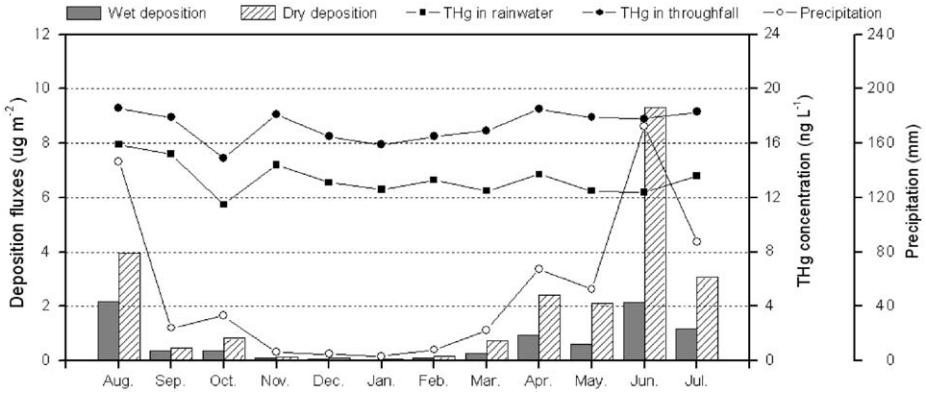

Fig. 4. Monthly wet/dry deposition flux, total Hg concentrations in rainwater/throughfall samples, and precipitation at Changbai area.

3.3.1. *Wet deposition flux*

Fig. 4 displays all the observational and experimental data including THg concentrations in rainwater/throughfall, monthly precipitation and wet/dry deposition fluxes. THg concentrations in rainwater samples ranged from 11.5 to 15.9 ng L^{-1}, while THg concentrations in throughfall samples were 14.9–18.6 ng L^{-1}, which were similar to Hg concentrations in rain of Great Lakes region (Hall et al., 2005). Thus, annual wet deposition flux of atmospheric Hg based on Eq. (1) was calculated to be 8.4 μg m^{-2}. This value is similar to those measured at the experimental lake area in Northwestern Ontario (St. Louis et al., 2001), a rural site in Athens (Yatavelli et al., 2006) and the state of New York (Lai et al., 2007). THg concentrations did not show a seasonal fluctuation, so that the variability of wet depositional flux is directly depended on monthly precipitations. Wet depositional flux in the rainy season (May–August) was calculated as 7.0 μg m^{-2}, which contributed 84% of the annual total wet deposition, and wet scavenging during this season may be responsible for the low Hgp concentrations.

3.3.2. *Dry deposition flux*

Besides scavenging by rain, Hg in air also can enter terrestrial and aquatic ecosystems through gravity deposition, atmospheric diffusion and other processes. There is not too much precipitation in northeastern China, thus, dry deposition is an important physical process. Thus, annual dry depositional flux based on Eq. (2) was calculated to be 16.5 μg m^{-2} a^{-1}. The lowest seasonal dry depositional flux was in winter, while fluxes in spring and fall were a little higher. Higher THg concentrations and plentiful rainfall in summer contributed to the most depositional flux (approximately 70% of total depositional flux) compared to other seasons. Mason et al. (2000) reported winter deposition constituted a similar fraction of total deposition (10–20%) for MDN sites and other eastern seaboard locations. Similarly, the depositional flux in winter (December–February) was less than 10% of the total flux. This difference is potentially due to: (1) less efficient scavenging of particles from the atmosphere by snow, as Hg concentrations in snow samples are similar to rainwater samples; or (2) lower temperature would hinder atmospheric photochemical reactions. Moreover, there is a significant correlation between wet deposition flux and dry deposition flux ($r = 0.893$, $p < 0.001$). The wet and dry deposition fluxes showed an apparent correlation with rainfall ($R^2 = 0.985/0.879$, $p < 0.001$) as displayed in Fig. 5.

3.3.3. *Modeled dry deposition flux*

Dry depositional velocity is a most important factor for estimating depositional flux in the modeled method. The dry depositional velocity depends on meteorological parameters (i.e. wind speed, relative humidity, and ambient temperature), particle characteristics and other factors; and it is difficult to determine or estimate the dry depositional velocity accurately. Ordinarily, a depositional velocity of coarse particle is higher than that of fine particles (Davidson et al., 1985). Changbai Mountain area is affected by pollution from coal burning for domestic usages and so that we selected a representative depositional velocity as 0.5 cm s^{-1} (GESAMP, 1989; Lamborg et al., 1995). Assuming the

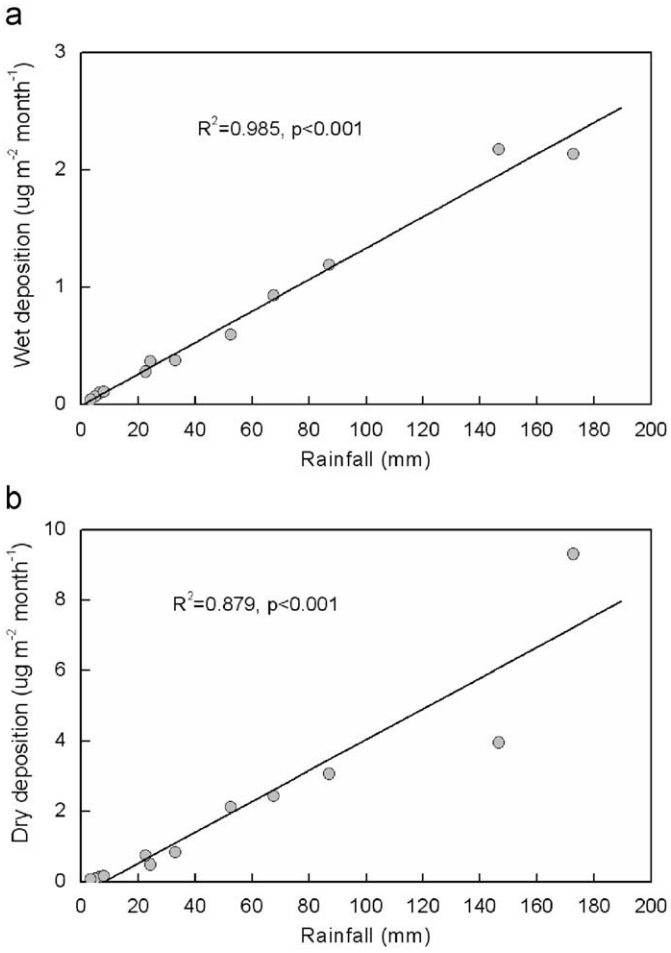

Fig. 5. Relationship between deposition flux and monthly rainfall at Changbai area.

total particulate Hg (TPM) concentration is 128 pg m^{-3}, then 60% of Hgp < 2.5 μm, (77 pg m^{-3}) and thus 40% of Hgp > 2.5 μm (51 pg m^{-3}). Annual dry depositional flux at study site based on Eq. (3) was modeled to be 20.2 μg m^{-2} a^{-1}, which is similar to the values reported in some areas in central and northern Europe (17.5 μg m^{-2} a^{-1}) (Petersen et al., 1995), but lower than those reported for Brazil (Silva-Filho et al., 2006). Compared to the measured dry depositional flux stated in Section 3.3.2, the modeled value is 18% higher mainly due to the uncertainty of dry depositional velocity, which may vary in different places (Lamborg et al., 1995).

4. Conclusions

Based on our study of atmospheric Hg species in Changbai Mountain area from August 2005 to July 2006, the mean concentrations of RGM and Hgp are 65 and 77 pg m^{-3}. Compared to measurements of atmospheric Hg in the Northern Hemisphere, RGM and Hgp levels in Changbai area are significantly elevated. Large values for standard deviation for RGM and Hgp indicate a fast reactivity and a low residence time. Results indicated great seasonal differences, with much lower concentrations in summer compared to other seasons. Low RGM and Hgp levels in summer are not only attributed to scavenging by rainfall but also due to low local Hg emissions. Wet depositional flux in Changbai area was calculated to be 8.4 μg m^{-2} a^{-1}, and dry deposition flux was estimated to be 16.5 μg m^{-2} a^{-1} according to a throughfall method, and 20.2 μg m^{-2} a^{-1} using a model method.

Acknowledgments

Special thanks to Canada Foundation for Innovation (CFI), Ontario Innovation Trust for providing the Hg-monitoring system.

References

Berg, T., Sekkesaeter, S., Steinnes, E., Valdal, A.K., Wibetoe, G., 2003. Springtime depletion of mercury in the European Arctic as observed at Svalbard. Sci. Total Environ. 304, 43–51.
Cohen, M., Artz, R., Draxler, R., Miller, P., Poissant, L., Niemi, D., Ratte, D., Deslauriers, M., Duval, R., Laurin, R., Slotnick, J., Nettesheim, T., McDonald, J., 2004. Modeling the atmospheric transport and deposition of mercury to the Great Lakes. Environ. Res. 95, 247–265.
Davidson, C.I., Lindberg, S.E., Schmidt, J., 1985. Dry deposition of sulfate onto surrogate surface. J. Geophys. Res. 90, 2121–2128.
Ericksen, J.A., Gustin, M.S., Lindberg, S.E., Olund, S.D., Krabbenhoft, D.P., 2005. Assessing the potential for Re-emission of mercury deposited in precipitation from arid soils using a stable isotope. Environ. Sci. Technol. 39, 8001–8007.
Fitzgerald, W.F., Manson, R.P., Vandal, G.M., 1991. Atmosphere cycling and air–water exchange of Hg over mid-continental Lacustrine regions. Water Air Soil Pollut. 56, 745–767.
Fu, X., Feng, X., Zhu, W., Zheng, W., Wang, S., Lu, J., 2008. Total particulate and reactive gaseous mercury in ambient air on the eastern slope of the Mt. Gongga area, China. Appl. Geochem. 23, 408–418.
Gabriel, M., Williamson, D., Brooks, S., Lindberg, S., 2005. Atmospheric speciation of mercury in two contrasting Southeastern US airsheds. Atmos. Environ. 39, 4947–4958.
GESAMP (Group of Experts on Scientific Aspects of Marine Pollution) Working Group 14, 1989. The atmospheric input of trace species to the world ocean. Rep. Stud. 38, World Meteorological Organization, Geneva, pp. 35.
Hall, B.D., Manolopoulos, H., Hurley, J.P., Schauer, J., St. Louis, V.L., Kenski, D., Graydon, J., Babiarz, C.L., Cleckner, L.B., Keeler, G.J., 2005. Methyl and total mercury in precipitation in the Great Lakes region. Atmos. Environ. 39, 7557–7569.
Han, Y.J., Holsen, T.M., Lai, S.O., Hopke, P.K., Yi, S.M., Liu, W., Pagano, J., Falanga, L., Milligan, M., Andolina, C., 2004. Atmospheric gaseous mercury concentrations in New York State: relationships with meteorological data and other pollutants. Atmos. Environ. 38, 6431–6446.
Hicks, B.B., Baldocchi, D.D., Meyers, T.P., Hosker, R.P., Matt, D.R., 1987. A preliminary multiple resistance routine for deriving deposition velocities from measured quantities. Water Air Soil Pollut. 36, 311–330.
Lai, S., Holsen, T.M., Hopke, P.K., Liu, P., 2007. Wet deposition of mercury at a New York state rural site: concentrations, fluxes, and source areas. Atmos. Environ. 41, 4337–4348.
Lamborg, C.H, Fitzgerald, W.F, Vandal, G.M., 1995. Atmosphere mercury in northern Wisconsin: sources and species. Water Air Soil Pollut. 80, 189–198.
Landis, M.S., Keeler, G.J., 2002. Atmospheric mercury deposition to Lake Michigan during the Lake Michigan Mass Balance Study. Environ. Sci. Technol. 36, 4518–4524.
Landis, M.S., Stevens, R.K., Schaedlich, F., Prestbo, E., 2002. Development and characterization of an annular denuder methodology for the measurement of divalent inorganic reactive gaseous mercury in ambient air. Environ. Sci. Technol. 36, 3000–3009.
Lindberg, S.E., Meyers, T.P., Taylor, G.E., Turner, R.R., Schroeder, W.H., 1992. Atmosphere surface exchange of mercury in a forest: results of modeling and gradient approaches. J. Geophys. Res 97, 2519–2528.
Lindberg, S.E., Owens, J.G., Stratton, W., 1994. Application of throughfall methods to estimate dry deposition of mercury. In: Watras, C.J., Huckabee, J.W. (Eds.), Mercury Pollution: Integration and Synthesis. Lewis Publishers, Palo Alto, pp. 261–271.
Lindberg, S.E., Stratton, W.J., 1998. Atmospheric speciation concentrations and behavior of reactive gaseous mercury in ambient air. Environ. Sci. Technol. 32, 49–57.
Lindberg, S., Bolluck, R., Ebinghaus, R., Engstrom, D., Feng, X., Fitzgerald, W., Pirrone, N., Prestbo, E., Seigneur, C., 2007. A synthesis of progress and uncertainties in attributing the sources of mercury in deposition. Ambio 36, 19–32.
Liu, B., Keeler, G.J., Dvonch, J.T., Barres, J.A., Lynam, M.M., Marsik, F.J., Morgan, J.T., 2007. Temporal variability of mercury speciation in urban air. Atmos. Environ. 41, 1911–1923.
Lu, J., Schroeder, W.H., 2004. Annual time-series of total filterable atmospheric mercury concentrations in the Arctic. Tellus 56B, 213–222.
Mason, R.P., Sullivan, K.A., 1997. Mercury in Lake Michigan. Environ. Sci. Technol. 31, 942–947.
Mason, R.P., Lawson, N.M., Sullivan, K.A., 1997. The concentration, speciation and sources of mercury in Chesapeake Bay precipitation. Atmos. Environ. 31, 3541–3550.
Mason, R.P., Lawson, N.M., Sheu, G.R., 2000. Annual and seasonal trends in mercury deposition in Maryland. Atmos. Environ. 34, 1691–1701.
Oslo and Paris Commission, 1998. JAMP Guidelines for the sampling and analysis of mercury in air and precipitation. Joint Assessment and Monitoring Programme (JAMP), 1–20.
Pacyna, E.G., Pacyna, J.M., 2002. Global emission of mercury from anthropogenic sources in 1995. Water Air Soil Pollut. 137, 149–165.
Petersen, G., Iverfeldt, A., Munthe, J., 1995. Atmospheric mercury species over Central and Northern Europe model calculations and comparison with observations from the Nordic Air and Precipitation Network for 1987 and 1988. Atmos. Environ. 29, 47–67.
Pirrone, N., Keeler, G.J., Warner, P.O., 1995. Trends of ambient concentrations and deposition fluxes of particulate trace metals in Detroit from 1982 to 1992. Sci. Total Environ. 162, 43–61.
Poissant, L., Pilote, M., Xu, X., Zhang, H., Beauvais, C., 2004. Atmospheric mercury speciation and deposition in the Bay St. Francois wetlands. J. Geophys. Res 109, D11301.
Poissant, L., Pilote, M., Beauvais, C., Constant, P., Zhang, H.H., 2005. A year of continuous measurements of three atmospheric mercury species (GEM, RGM and Hg-P) in southern Québec, Canada. Atmos. Environ. 39, 1275–1287.
Ryaboshapko, A., Bullock, R., Ebinghaus, R., Ilyin, I., Lohman, K., Munthe, J., Petersen, G., Seigneur, C., Wangberg, I., 2002. Comparison of mercury chemistry models. Atmos. Environ. 36, 3881–3898.
Sakata, M., Marumoto, K., 2005. Wet and dry deposition fluxes of mercury in Japan. Atmos. Environ. 39, 3139–3146.
Sakata, M., Asakura, K., 2007. Estimating contribution of precipitation scavenging of atmospheric particulate mercury to mercury wet deposition in Japan. Atmos. Environ. 41, 1669–1680.
Sheu, G.R., Mason, R.P., 2001. An examination of methods for the measurements of reactive gaseous mercury in the atmosphere. Environ. Sci. Technol. 35, 1209–1216.
Silva-Filho, E.V., Machado, W., Oliveira, R.R., Sella, S.M., Lacerda, L.D., 2006. Mercury deposition through litterfall in an Atlantic Forest at Ilha Grande, Southeast Brazil. Chemos 65, 2477–2484.
Louis, V.L., Rudd, J.W.M., Kelly, C.A., Hall, B.D., Rolfhus, K.R., Scott, K.J., Lindberg, S.E., Dong, W.J., 2001. Importance of the forest canopy to flux of methylmercury and total mercury to boreal ecosystems. Environ. Sci. Technol. 35, 3089–3098.
Streets, D.G., Hao, J.M., Jiang, J.K., Chan, M., Tian, H.Z., Feng, X.B., 2005. Anthropogenic mercury emissions in China. Atmos. Environ. 39, 7789–7806.
Swain, E.B., Engstrom, D.R., Brigham, M.E., Henning, T.A., Brezonik, P.L., 1992. Increasing rates of atmospheric mercury deposition in midcontinental North America. Science 257, 784–787.
Tekran, 2001. Tekran Model 1130 Mercury Speciation Unit and Model 1135—Particulate Mercury Unit User Manual, Toronto, Canada.
US EPA, Method, 1631, 2001. Revision B: Mercury in Water by Oxidation, Purge and Trap, and Cold Vapor atomic Fluorescence Spectrometry. United States Environmental Protection Agency, pp. 1–33.
Wan, Q., Feng, X., Lu, J., Zheng, W., Song, X., Han, S., Xu, H., 2009. Atmospheric mercury in Changbai Mountain area, northeastern China I. The seasonal

distribution pattern of total gaseous mercury and its potential sources. Environ. Res. 109, 201–206.

Wu, Y., Wang, S., Streets, D.G., Hao, J., Chan, M., Jiang, J., 2006. Trends in anthropogenic mercury emissions in China from 1995 to 2003. Environ. Sci. Technol. 40, 5312–5318.

Yatavelli, R.N., Fahrnia, J.K., Kim, M., Crist, K.C., Vickers, C.D., Winter, S.E., Connell, D.P., 2006. Mercury, $PM_{2.5}$ and gaseous co-pollutants in the Ohio River Valley region: preliminary results from the Athens supersite. Atmos. Environ. 40, 6650–6665.